ELSEVIER

Journal of Chromatography A, 883 (2000) 231–248

JOURNAL OF CHROMATOGRAPHY A

www.elsevier.com/locate/chroma

Laser-induced dispersed fluorescence detection of polycyclic aromatic compounds in soil extracts separated by capillary electrochromatography

Michael G. Garguilo[*,1], David H. Thomas[1], Deon S. Anex[2], David J. Rakestraw[2]

Sandia National Laboratories, P.O. Box 969, Livermore, CA 94551-0969, USA

Received 29 December 1999; received in revised form 23 March 2000; accepted 24 March 2000

Abstract

Polycyclic aromatic hydrocarbons (PAHs) and nitrogen containing aromatic compounds (NCACs) are characterized in soil extracts and laboratory standards by capillary electrochromatography (CEC) with laser-induced dispersed fluorescence (LIDF) detection using a liquid-nitrogen cooled charge-coupled device detector. The LIDF detection technique provides information on compound identity and, when coupled with the high separation efficiencies of the CEC technique, proves useful in the analysis of complex mixtures. Differences in fluorescence spectra also provide a means of identifying co-eluting compounds by using deconvolution algorithms. Detection limits range from 0.5 to 96×10^{-10} *M* for selected PAHs and $0.9–3.7\times10^{-10}$ *M* for selected NCACs. Soil extracts are also injected onto the CEC column to evaluate chromatographic method performance with respect to complex samples and the ability to withstand exposure to environmental samples.

Keywords: Laser-induced dispersed fluorescence; Deconvolution; Soil extracts; Polynuclear aromatic compounds

1. Introduction

Identification and quantitation of multiple analytes in complex samples is essential in environmental restoration and monitoring, biomedical research, clinical diagnostics, and forensics. Scientific techniques and procedures are needed not only for the rapid and efficient separation of analytes for their positive identification, but also for the detection of analytes present in trace amounts. Separation and sensitive detection have been addressed previously in our lab using capillary electrochromatography (CEC) with non-dispersed laser-induced fluorescence (LIF) detection for the separation and detection of polycyclic aromatic hydrocarbons (PAHs) [1,2]. The analysis of PAHs, which are carcinogenic and toxic substances, is an important environmental problem [3].

This paper places an emphasis on the rapid and positive identification of individual analytes through spectral information obtained from sensitive dispersed fluorescence detection coupled to CEC, a separation technique having high efficiency. CEC has been shown to be a very powerful technique in

*Corresponding author.

[1]Present address: PE Biosystems, 850 Lincoln Centre Drive, Foster City, CA 94404, USA.

[2]Present address: Dionex Corporation, 1228 Titan Way, Sunnyvale, CA 94088, USA.

0021-9673/00/$ – see front matter
PII: S0021-9673(00)00409-X

separating neutral compounds and its advantages over μHPLC in terms of resolution and mechanical requirements have been reported [1,2,4–11]. CEC has several advantages over micellar electrokinetic capillary chromatography (MEKC), which has limited mobile phase composition, loadabiltiy, and versatility. The recent reports of polymer micelles and the use of higher organic modifier concentrations are addressing these important issues [12,13].

Wavelength dispersed detection coupled with capillary column separations is a very powerful analytical approach for identifying compounds in complex samples [14]. Several commercially available capillary electrophoresis (CE) instruments now incorporate diode array detectors so that the user can obtain absorbance spectra of separated compounds for identification purposes [15]. However, because of the extremely small pathlength presented by the capillary in both CE and CEC, detection using absorbance techniques is far less sensitive than fluorescence-based approaches. LIF has been shown to be a very sensitive detection scheme for analytes that either fluoresce natively [16–23] or that are tagged with fluorescent molecules [24,25]. This approach becomes even more powerful if the fluorescence is dispersed onto a charged-couple device (CCD) detector [26–31] and detailed spectral information is obtained for each analyte. Sweedler and coworkers have shown that laser-induced dispersed fluorescence (LIDF) in combination with CE allows sensitive detection and identification of analytes based on their different electrophoretic mobilities and different fluorescence spectra [32–36]. Recently, Sweedler and coworkers used LIDF in combination with CE to identify and separate more than 30 biological compounds from single neurons [32]. This work demonstrated the power of using LIDF in combination with high-performance separation techniques to analyze complex samples.

The fluorescence spectra for PAHs and nitrogen-containing aromatic compounds (NCACs) have structure that can significantly aid in their identification in standards and real samples. Novotny and coworkers employed a mercury-xenon arc lamp as an excitation source and an intensified linear photodiode array detector to obtain the detailed fluorescence spectra for several polycyclic aromatic compounds (PACs) that were separated using microcolumn high-performance liquid chromatography (μHPLC) [37–39]. The photodiode array detector was necessary for the identification of the fluorescent compounds in fossil fuels and other complex samples. Jalkian and Denton also dispersed fluorescence to obtain detailed emission spectra for several PACs separated by conventional HPLC [40]. The fluorescence spectra were collected using a CCD detector and a mercury pen lamp or deuterium lamp excitation source.

In this paper, LIDF detection is coupled with CEC and used to obtain the detailed fluorescence spectra for PAHs and NCACs as they elute from the column. Two optical designs are investigated and their performance is discussed. Limits of detection for selected compounds are determined. This paper also demonstrates the utility of using dispersed fluorescence in the deconvolution of coeluting peaks. The separation and sensitive detection of PAHs and NCACs in soil extracts is performed to evaluate the potential of LIDF in combination with CEC to rapidly identify analytes in complex environmental samples and to demonstrate the robustness of CEC in the analysis of real-world samples.

2. Experimental section

2.1. Dispersed fluorescence detection set-up

Fig. 1 shows a schematic of the dispersed fluorescence detection set-up. The 257-nm line of an intracavity-doubled argon ion laser (Coherent, Santa Clara, CA) was used to excite the PAHs and the NCACs. The separation capillaries were oriented horizontally, with the excitation laser beam approaching vertically from above. The laser beam was focused onto the window of packed fused-silica capillaries using a lens with a focal length (f) of 75 mm. All lenses used in the experiments described in this paper were UV-grade fused-silica plano-convex and had one-inch diameters. Fluorescence was collected using a system of lenses (Fig. 1, Scheme A) or a microscope and lens combination (Fig. 1, Scheme B). When a lens (f=25 mm) was used as the collection optic (see Fig. 1, Scheme A), the fluorescence was focused onto the slit of the monochromator with a second lens having an f of 100 mm. The second lens was chosen to match the

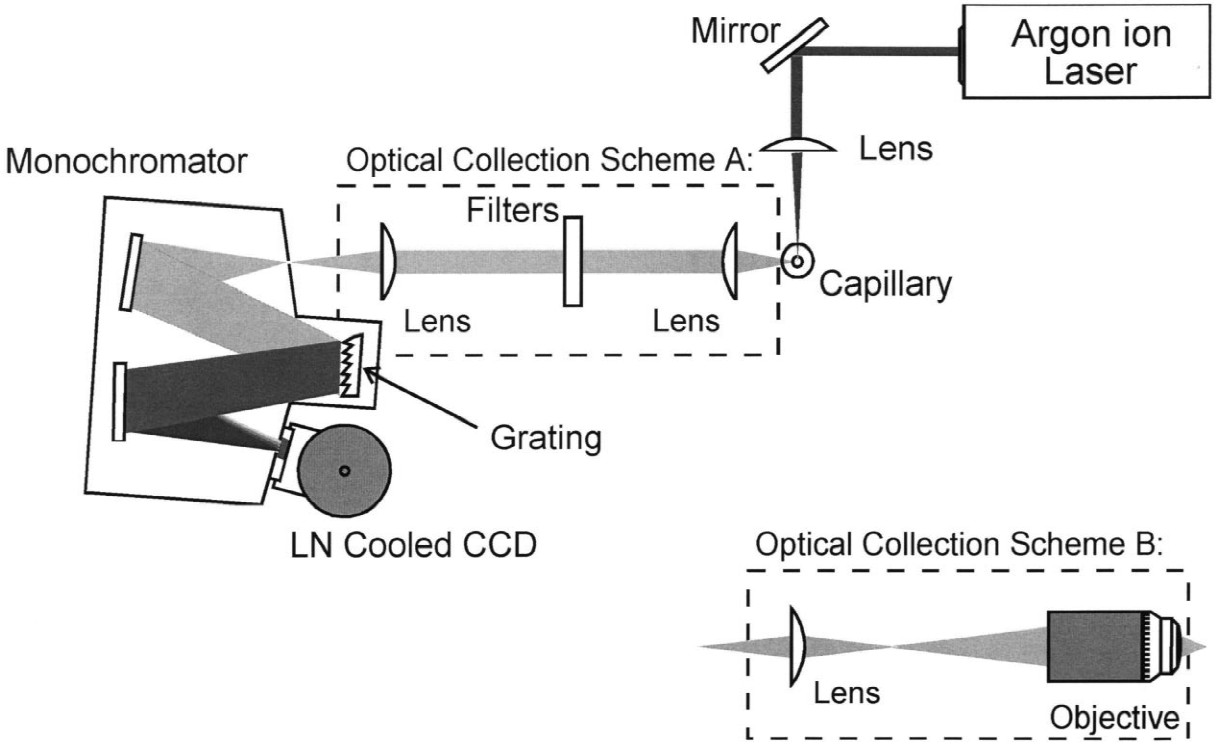

Fig. 1. Schematic diagram of the laser-induced dispersed fluorescence (LIDF) detection set-ups. A combination of UV lenses (Scheme A) or microscope objective and UV lens (Scheme B) is illustrated as the collection optics.

f-number of the monochromator ($f/\#=4$). The fluorescence filled the entire 1-in. diameter of the focusing lens. A pair of 280-nm long pass filters were placed in the path of the collected fluorescence prior to reaching the monochromator to reject the scattered laser light coming from the capillary.

In several experiments, the first lens was replaced with a high-numerical-aperture (NA) microscope objective (40× magnification, NA=0.85, 0.37 mm working distance; Technical Instruments, San Francisco, CA) having a short wavelength transmission cut-off at 320 nm (see Fig. 1, Scheme B). In these experiments, the fluorescence was focused onto the slit of the monochromator with a second lens having an *f* of 25 mm. The microscope objective formed an image (~4 mm high and~2 mm wide) 100 mm in front of the second lens. This image was refocused by the second lens onto the monochromator slit 40 mm beyond the lens. The fluorescence filled an area ~10 mm high and ~5 mm wide at this focusing lens. The long pass filters used with the lens as the collection optic were not necessary because of limited short wavelength transmission of the microscope objective. The collected fluorescence was dispersed by the monochromator (SPEX 270M; Instruments SA, Edison, NJ) using a 300 grooves/mm grating with a blaze angle optimized for 600 nm. The dispersed-fluorescence was detected with a liquid nitrogen-cooled CCD (1100×330 pixels; Princeton Instruments, Trenton, NJ). Data were collected from the CCD at 1 Hz using a PC and the manufacturer's software. A serial bin factor of 5 pixels and a parallel bin factor of 330 pixels were used to enhance signal-to-noise (S/N) while at the same time preserving spectral resolution (1.46 nm/superpixel).

2.2. CEC-separations and preparation of packed capillaries

Polyimide coated fused-silica capillaries were

purchased from Polymicro Technologies (Phoenix, AZ) and were used as received. Capillaries having inner diameters of 75–100 μm were electrokinetically packed with 3 μm octyldecylsilica (ODS) porous particles (SynChrom; Lafayette, IN) using a previously reported procedure [1]. The particles were washed several times with ACN and methanol prior to being packed into the fused-silica capillaries. This washing step was necessary to remove fluorescent contaminants from the particles and thus reduce the background fluorescence observed in the LIDF/CEC experiments. The washed 3 μm ODS particles were suspended in 100% methanol. To contain the particles in the capillaries during the electrokinetic packing procedure, an initial frit was made by sintering 5 μm silica paste with a microtorch. After placing the electrokinetically packed capillary on a HPLC pump and applying a pressure of ~4000 p.s.i., a second frit was made on column by sintering the 3 μm ODS particles with a resistively heated thermal wire stripper. The packed column was reversed on the HPLC pump so that any excess 3 μm ODS particles could be flushed out of the capillary and an inlet frit consisting of the 3 μm ODS material could be made using the thermal wire stripper while the column was still under high pressure. If a gap appeared during the making of the inlet frit, the packed capillary was immersed in a sonicator for ~5 min while still under high pressure. After sonication, another frit sintering attempt was made using the thermal wire stripper. The sonication and inlet frit sintering with the wire stripper were repeated until there was no visible gap in the packed column, which remained under high pressure throughout this procedure. The packed portion of the capillary was typically 25–35 cm in length, with the total length of the column being 40–50 cm. A window for excitation and detection was created ca. 2 mm after the packed section of the column, unless otherwise noted. Initially, a low voltage (1–2 kV) was applied across the packed column with the inlet and outlet of the capillary immersed in vials containing the specified mobile phase to condition the column for separations. High voltage (~25 kV) was applied across the packed column to perform the separations of the PAHs and NCACs in the standard mixtures and soil extracts.

2.3. Chemicals and materials

Tris(hydroxymethyl)aminomethane (TRIS, reagent grade), sodium tetraborate, acetonitrile (HPLC Grade), and methanol were purchased from Sigma (St. Louis, MO). Mobile phases were prepared by mixing a specified volume of acetonitrile (ACN) with either a 2 m*M* TRIS or 5 m*M* TRIS solution (pH 8.0) or a 4 m*M* sodium tetraborate solution (pH 9.0). All solutions were made using 18 MΩ·cm deionized water from a Labconco (Kansas City, MO) purification system. The soil extracts and individual NCACs were provided by Dr. William C. Brumley at the US Environmental Protection Agency. A description of the procedures for preparing the soil extracts is available in an earlier publication [3]. The as-received soil extracts were diluted 10–100 fold with the mobile phase used for the CEC runs. The individual NCACs were received as solids and were first dissolved in ACN before being diluted with the mobile phase. The mixtures of NCACs were made using the solutions containing the individual NCACs. The priority pollutant PAH mixture (Standard Reference Material 1647d) in ACN was purchased from the National Institute of Standards and Technology (NIST; Gaithersburg, MD). This mixture was diluted with the mobile phase and used as the PAH standard. The mobile phase was degassed by sonication on a day-to-day basis prior to CEC experiments.

3. Results and discussion

Various parameters are known to affect the resolution of the spectra obtained using dispersed fluorescence detection schemes. The monochromator slit width and diffraction order of the grating were varied to determine the optimum conditions under which to identify PAHs and NCACs in environmental samples using CEC and LIDF detection.

3.1. LIDF detection and CEC separation of PAH standards — varying monochromator slit width

Fig. 2 shows the separation by CEC with LIDF detection of a standard mixture of three PAHs (naphthalene, anthracene, and pyrene) and the effect

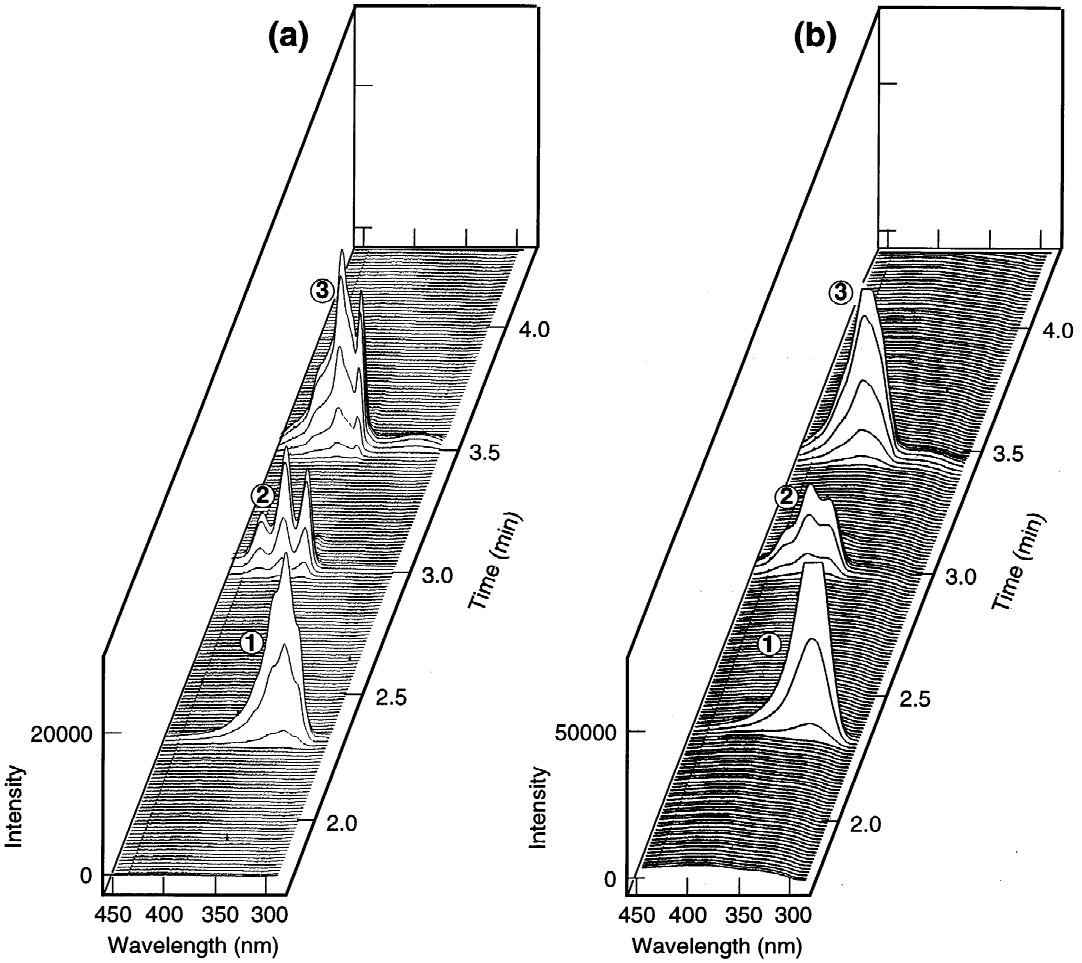

Fig. 2. LIDF spectra of (1) naphthalene, (2) anthracene, and (3) pyrene separated by capillary electrochromatography (CEC). The fluorescence spectra were obtained using monochromator slit widths of (a) 400 μm and (b) 2000 μm. Dispersed fluorescence was collected using the grating in second order. The fluorescence was collected using the system of UV lenses shown in Fig. 1, Scheme A. The PAHs were separated by applying 20 kV across a ~40-cm long fused-silica capillary (75-μm inner diameter) packed with ~13 cm of 3-μm ODS porous silica particles and using a mobile phase composition of 70% ACN and 30% 2 m*M* TRIS. A 5 s, 5 kV electrokinetic injection was used to introduce the sample onto the column.

of monochromator slit width on spectral resolution for each PAH. The detection window was located ca. 7 cm from the outlet frit of the packing. The length of open column between the frit and the detection window was unusually long in this case because of the short length of packing and the overall length of capillary required for the detection system. The fluorescence from each PAH standard, as it passed by the window, was collected using the system of UV lenses (Fig. 1, Scheme A), dispersed by the monochromator, and recorded by the CCD camera. The grating was used in second order to increase spectral resolution.

Fig. 2a shows the data obtained for the three PAHs using a monochromator slit width of 400 μm, while Fig. 2b shows the data obtained using a slit width of 2000 μm. As expected, as the slit width of the monochromator was increased, the spectral resolution decreased. This loss in spectral resolution is clearly seen in the fluorescence spectra for both

anthracene (peak 2) and pyrene (peak 3). As expected, the intensity also increased when the slit width of the monochromator increased. The fluorescence peak intensity for each of the PAHs increased by a factor of ~2 when the slit width of the monochromator was increased by a factor of 5. This increase in intensity leads to 1.49 ± 0.21 ($n=12$) times lower detection limits (close to the expected square root of 2) [41] for the individual PAH standards. Detection limits for several PAH standards are reported later in this paper.

3.2. First order versus second order dispersed fluorescence collection

The orders of diffraction (i.e., first and second orders) collected from the grating are also known to affect the spectral resolution and measured intensity of the fluorescence. Fig. 3 shows the first order and second order dispersed fluorescence of the first 13 eluting PAHs in the NIST standard mixture containing 16 total PAH standards. Only the first 12 min of the electrochromatogram are shown so that more details of the spectra for the first few eluting PAHs can be displayed in Fig. 3. The full separation was completed in 25 min. The fluorescence was collected using the system of UV lenses shown in Fig. 1, Scheme A. A monochromator slit width of 400 μm was used to resolve spectral features.

Fig. 3a shows the two-dimensional (retention time and fluorescence wavelength) data for the first 13 eluting PAHs using the grating in first order. Fig. 3b shows data obtained under similar separation conditions while using the grating in second order. The insets in Fig. 3a and b show the chromatograms obtained by integrating the entire spectral region. All of the chromatogram insets shown in this paper were obtained in the same manner. In general, slightly more spectral information and detail were obtained when using the grating in second order. In some cases, there is no advantage to using second order over first order. For example, the fluorescence spectra for fluoranthene (peak 7) and benzo[*b*]fluoranthene (peak 11) are broad and featureless in both second order and first order. Using the grating in first order may be important if both spectral information and high sensitivity are necessary. It is interesting to note that there are variations in the intensities for the PAHs in the first and second order spectra. This is clearly seen for naphthalene (peak 1), fluorene and acenaphthene (peaks 3 and 4), fluoranthene (peak 7), and benzo[*b*]fluoranthene (peak 11) in the chromatograms shown as insets in Fig. 3. This can be explained by considering the blaze angle of the grating used to collect the data. The grating was blazed at an angle that made the collection of fluorescence most efficient at 600 nm. Spectra were not corrected for grating efficiency. With this grating, second order can be used to maximize spectral information with comparable sensitivity to first order. If more sensitivity is desired, the grating could be replaced with one that was more efficient at the shorter, UV wavelengths (e.g. 370 nm).

3.3. Spectral deconvolution of co-eluting compounds

Even though CEC is a very powerful technique in separating the PAH standards in the NIST mixture, it is necessary to vary the running conditions (i.e., perform a gradient or run multiple capillaries where different conditions are used for each capillary) to quickly separate all 16 PAHs when a 3 μm support is used. An attractive alternative to gradient elution or multiple capillary techniques for PAH analysis by CEC is to use differences in the fluorescence spectra to distinguish co-eluting PAHs. A simple linear curve-fitting program written in-house was used to deconvolute and determine the ratio of two PAHs that co-eluted in the chromatograms shown in Fig. 3. Under the running conditions used to obtain Fig. 3, acenaphthene and fluorene (peaks 3 and 4, respectively) co-elute. To obtain the fluorescence spectra for each PAH using the LIDF set-up, solutions of the individual PAHs were flushed through an open fused-silica capillary. Fig. 4a and b show the fluorescence spectra for acenaphthene and fluorene, respectively. Second order dispersed fluorescence collection and a slit width of 100 μm were used to resolve the spectral features for each PAH. The fluorescence was collected using the system of UV lenses shown in Fig. 1, Scheme A.

In order for the deconvolution program to work effectively, the spectra for the two co-eluting species must be different. Fig. 4a and b show that the spectra for acenaphthene and fluorene are different in both

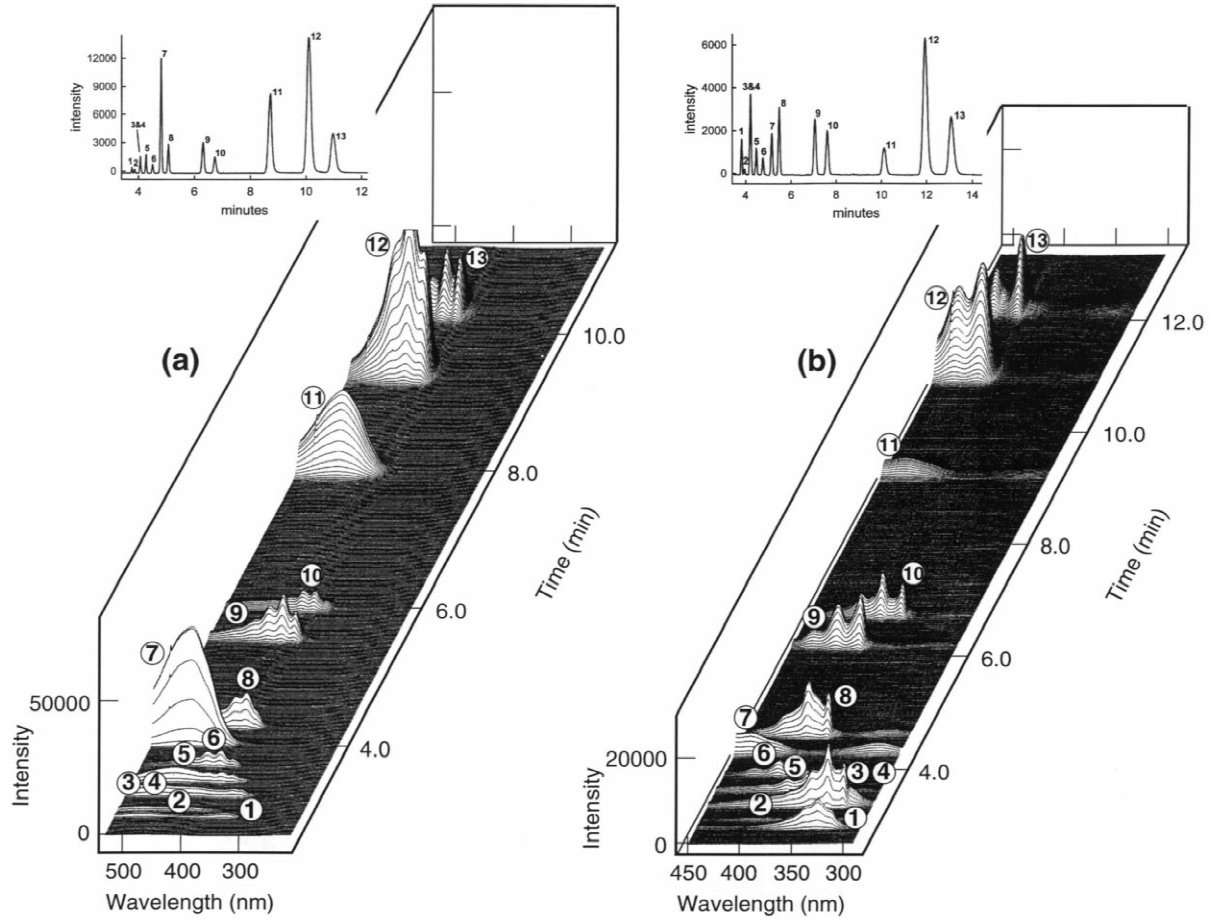

Fig. 3. LIDF spectra and CEC separation of PAH standards: (1) naphthalene, (2) acenaphthylene, (3) acenaphthene, (4) fluorene, (5) phenanthrene, (6) anthracene, (7) fluoranthene, (8) pyrene, (9) benz[*a*]anthracene, (10) chrysene, (11) benzo[*b*]fluoranthene, (12) benzo[*k*]fluoranthene, and (13) benzo[*a*]pyrene. Fluorescence was collected using the grating in (a) first order and (b) second order. A monochromator slit width of 400 μm was used to obtain the spectra. The fluorescence was collected using the system of UV lenses shown in Fig. 1, Scheme A. The insets show the chromatograms obtained by integrating the entire spectral region. The standard solution was separated using a CEC column made with a fused-silica capillary (75-μm inner diameter, ~40 cm long) having a packed length of ~13 cm and using a mobile phase composition of 70% ACN and 30% 2 m*M* TRIS. A separation voltage of 20 kV was applied across the capillary and a 2 s, 20 kV electrokinetic injection was used to introduce the NIST sample (diluted 10-fold in the mobile phase) onto the column.

wavelength position and structure. Fig. 5a shows the experimental chromatogram (solid line) and Fig. 5b, c, and d show the spectral data (open circles) from Fig. 3b at specific times during the separation. Fig. 5a shows the chromatogram (solid line) for acenaphthene and fluorene, showing that the two PAHs co-elute. The dashed and dotted lines in the plot represent the deconvoluted components for acenaphthene and fluorene, respectively. The arrows labeled b, c, and d in Fig. 5a represent the times at which the spectral data shown in Fig. 5b, c, and d were obtained. In Fig. 5b, c, and d the experimental spectral data (open circles) are fit with the results (dash-dotted lines) from the deconvolution program. The dashed and dotted lines in Fig. 5c represent the deconvoluted components for acenaphthene and fluorene, respectively. These lines are not shown in Fig. 5b or d since only one component, either acenaphthene or fluorene, was present at these times during the separation.

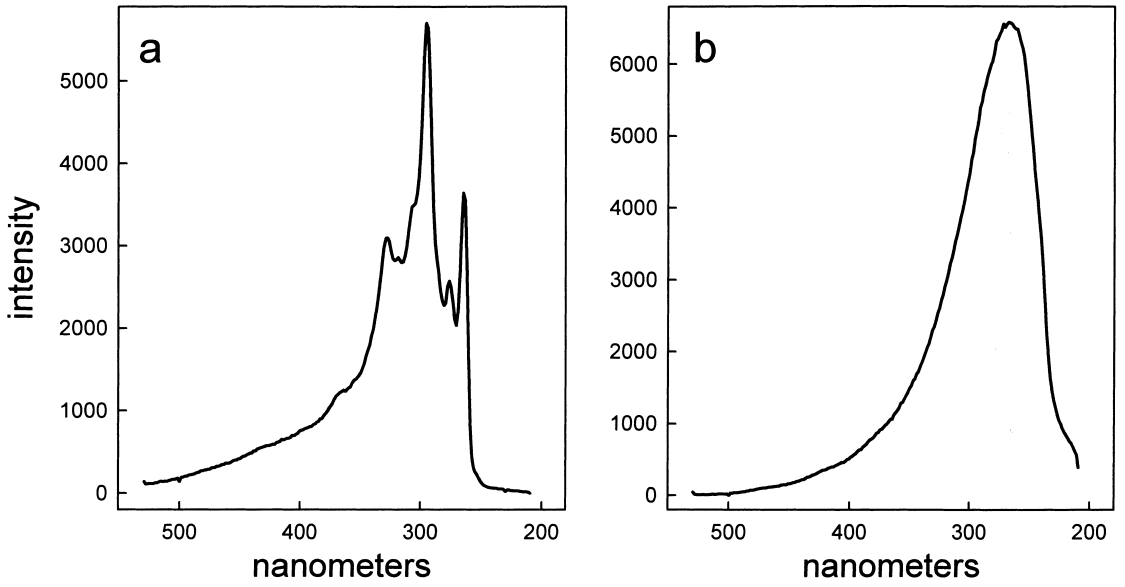

Fig. 4. Second order dispersed fluorescence spectra of (a) acenaphthene and (b) fluorene. A monochromator slit width of 100 μm was used to obtain the spectra. The fluorescence was collected using the system of UV lenses shown in Fig. 1, Scheme A. Separate solutions for each PAH were flushed through an open fused-silica capillary.

The results obtained with the deconvolution program can be used to determine the ratio of these components in the mix. The integrated areas under the spectra for acenaphthene (10 m*M*) and fluorene (10 m*M*), shown in Fig. 4, and the integrated areas under the deconvoluted spectra were used to determine that the NIST standard had an acenaphthene to fluorene ratio of 4.35:1. NIST reports that the sample contains a 4.49:1 ratio. The 3% error in the ratio shows the effectiveness of the deconvolution technique in quickly determining the relative amounts of two co-eluting species in a complex mixture.

3.4. Microscope objective as fluorescence collection optic

All of the previous results were obtained using an UV lens as the fluorescence collection optic. To improve the fluorescence collection efficiency of the system, the UV lens was replaced with the 40× microscope objective (see Fig. 1, Scheme B). The CEC separation with second order dispersed fluorescence detection for all 16 PAHs (acenaphthene and fluorene still co-elute under these running conditions) in the NIST standard were obtained (data not shown) and compared to the data collected with the system of UV lenses. A monochromator slit width of 100 μm was used to reduce the amount of light entering the system to prevent overloading the CCD camera. This reduction was necessary because the microscope objective led to a higher background due its higher collection efficiency.

There are no significant differences in the spectral features for each PAH when compared to the spectra obtained with the UV lens as the collection optic shown in Fig. 3. However, the peak intensities for the spectra of the PAHs obtained using the microscope objective as the collection optic were ~2 times higher than the peak intensities for the corresponding spectra obtained using the UV lens as the collection optic. By considering relative quantities injected and slit widths, it can be shown that there is significantly higher collection efficiency with the microscope objective than with the lens. For the experiments employing the microscope objective, the amount of the NIST standard injected onto the column was 1/5 the amount injected to obtain the results using the lens. In addition, the slit width on the monochromator was a factor of 4 narrower when the data

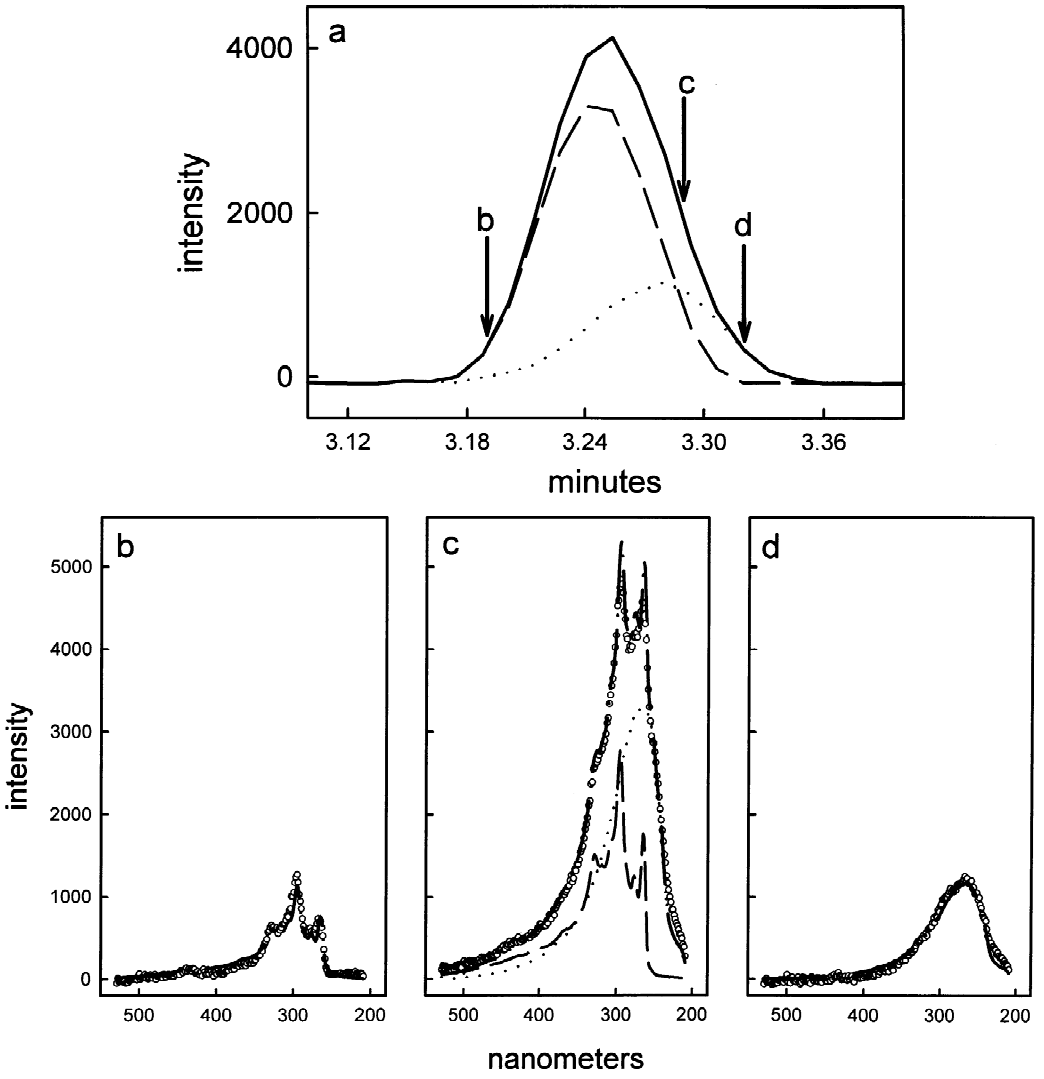

Fig. 5. Chromatogram (a) and spectra (b, c, and d) for co-eluting peaks 3 and 4 from Fig. 3b. In panel (a), the chromatogram is shown by the solid line with its deconvoluted components, acenaphthene (dashed line) and fluorene (dotted line). The arrows indicate the times corresponding to the spectra shown in panels (b), (c), and (d). The spectra (open circles) were collected in second order at 3.19, 3.29, and 3.32 min and fit with results (dash-dotted lines) from a deconvolution program. The dashed line and dotted line in panel (c) represent the deconvoluted components acenaphthene and fluorene, respectively.

using the microscope objective were collected in comparison to the data obtained using the lens. These results indicate that the fluorescence collection efficiency is enhanced by more than an order of magnitude with the replacement of the UV lens by the microscope objective as the collection optic. In the case when high fluorescence background is present, however, the full gains of enhanced collection efficiency are offset partially by the need to attenuate the signal. This is further discussed below with respect to limits of detection.

3.5. Detection limits for PAHs

Although this paper places an emphasis on the identification of compounds in complex mixtures

Table 1
Detection limits (d.l.) for PAHs using UV-LIDF detection[a]

PAH(λ_{max})	d.l. ($\times 10^{-10}$ M)		
	I	II	III
Naphthalene (344 nm)	38.1	26.4	84.6
Anthracene (406 nm)	3.32	1.88	2.12
Pyrene (393 nm)	11.8	5.73	8.49
Chrysene (393 nm)	4.81	2.30	4.97
benzo[*k*]fluoranthene (433 nm)	1.62	0.83	0.51

[a] Results were obtained using UV-LIDF detection with an UV-lens as the collection optic. UV-LIDF detection was performed using (I, II) second order and (III) first order diffraction from the grating, a wavelength integration of (1) 320 nm, (II) 70 nm or (III) 60 nm, and a monochromator slit width of 2000 μm.

through differences in spectral features, it is also important to understand the impact of LIDF on detection sensitivity. Table 1 shows the detection limits ($S/N=3$) for 5 of the 16 PAH standards separated using CEC and the dispersed fluorescence set-up with the UV lens as the collection optic (Fig. 1, Scheme A). Detection limits of the dispersed fluorescence set-up were determined using a monochromator slit width of 2000 μm and different wavelength integration ranges. The number in parenthesis next to the name of each PAH in Table 1 represent the wavelength maximum around which the integration was performed.

The fluorescence signal levels increased faster than the noise levels as the monochromator slit widths were widened over the range of 100–2000 μm, leading to an improvement in detection limits at a slit width of 2000 μm. Detection limits also improved by narrowing the wavelength region over which the integration was performed so that more background noise could be discriminated against. Similar background noise discrimination was observed when performing the LIF experiments using non-dispersive fluorescence collection and a 70-nm band-pass filter [1]. Overall, the results in Table 1 show that the detection limits observed using the dispersed fluorescence set-up are generally higher than those reported using the non-dispersed, LIF-photomultiplier tube (LIF-PMT) set-up [1].

Unfortunately, the dispersed and non-dispersed LIF experiments are not directly comparable. The overall higher detection limits observed using the dispersed fluorescence set-up in comparison to the LIF-PMT set-up are due to the background fluorescence (and associated noise) from the contaminants of the CEC column. These unidentified fluorescent contaminants were present on the bulk column material and were only partially removed with multiple washings using ACN and methanol. These contaminants were present during the current experiments but not during the experiments from which the detection limits using the LIF-PMT set-up were determined. The background fluorescence had a wavelength range of 350–530 nm and a wavelength maximum of 450 nm when employing the system of UV lenses. The background fluorescence had a wavelength range of 310–530 nm and a wavelength maximum of 430 nm when using the microscope objective as the collection optic. The difference between the spectra for the background fluorescence obtained with the two different collection optics is most likely due to a contribution to the fluorescence from the microscope objective itself.

Even with a ten-fold improvement in collection efficiency using the microscope objective, the detection limits were not better compared with using the lens as the collection optic. It is important to note that 1/20 of the laser power was used in the determination of the detection limits during the experiments using the microscope objective. It was necessary to use over an order of magnitude less laser power since the background fluorescence was significantly larger when performing the experiments employing the microscope objective. This was mainly due to an increase in the collection efficiency of the fluorescence from the contaminants. This explains why the detection limits obtained with the UV lens as the collection optic were similar to those obtained with the microscope objective as the collection optic. The increased collection efficiency observed with the microscope objective was offset by the necessary reduction in laser power. Significantly better performance can be expected with the microscope objective under conditions where the background fluorescence levels are low enough so that the excitation laser does not have to be attenuated.

Complete removal of the fluorescent contaminants beyond multiple washings was not pursued since the major theme of this paper is the identification of compounds based on their spectral features and not detection limits. However, the detection limits re-

ported for the PAHs observed using the dispersed fluorescence set-up are still very low (only an order of magnitude or less higher than those reported using the LIF-PMT set-up) and with optimization and removal of the fluorescent contaminants could reach levels lower than those reported for the LIF-PMT set-up. This demonstrates the potential of the dispersed fluorescence set-up in not only identifying compounds based on their spectral features but also detecting trace amounts of those compounds in complex samples.

3.6. LIDF detection and CEC separation of NCAC standards

The same dispersed fluorescence set-up with the microscope objective as the collection optic (Fig. 1, Scheme B) was used to identify nitrogen-containing aromatic compounds (NCACs) in a standard mix. Fig. 6 shows the separation and the two-dimensional data for 7 NCACs using the grating in second order. The inlet of the fused-silica capillary was rinsed with 100% ACN after each injection to remove trapped and adsorbed fluorescent compounds that caused the background of the chromatogram to fluctuate dramatically and caused tailing in the chromatographic peaks. A monochromator slit width of 100 μm was again used to limit the amount of light entering the monochromator from the high fluorescence background.

The inset in Fig. 6 shows the chromatogram for the same separation of the NCACs obtained by integrating the entire spectral region. The retention times for the NCACs are very short compared to those of the 16 PAHs. Table 2 shows the detection limits for three of the NCACs shown in Fig. 6. The detection limits are similar to those determined for the PAHs.

3.7. LIDF detection and CEC separation of PAHs and NCACs in a standard mix

To make a more challenging sample that contains compounds expected in creosote-contaminated soil extracts, the 16 PAH NIST standard solution was mixed with the 7 NCAC standard solution and the resulting standard mix was analyzed. This test also demonstrated how the dispersed fluorescence set-up performs under circumstances where there is more than one set of co-eluting compounds, which will likely occur when attempting to separate and identify compounds in real samples. Fig. 7 shows the separation and the two-dimensional data for the first 14 eluting compounds in the 23 compound standard mix of PAHs and NCACs using the grating in second order. Under these running conditions, the last of the 23 compounds eluted in ~90 min. The inset in Fig. 7 shows the chromatogram for the first 14 eluting compounds obtained by integrating the entire spectral region. The fluorescence was collected using the UV lens and microscope objective combination shown in Fig. 1, Scheme B. A monochromator slit width of 100 μm was used.

At the percentage of organic modifier used in the mobile phase for this separation, two sets of peaks co-elute and can not be identified or quantified using conventional retention matching methods. Without dispersed fluorescence to aid in identifying these two sets of co-eluting peaks, the mobile phase composition would have to be changed, most likely more than once, to separate the compounds from one another. Compound identification by spiking and retention matching techniques would then require injecting each of the 23 compounds individually. The dispersed fluorescence set-up only requires a base knowledge of what the spectra look like for each of the different compounds and a deconvolution program. This is extremely advantageous when trying to rapidly identify multiple compounds in a real sample.

3.8. Identification of PAHs and NCACs in environmental extracts

To show the capabilities of dispersed fluorescence detection in identifying PAHs and NCACs in a real environmental sample, a creosote-contaminated soil extract was injected onto a CEC column. Fig. 8 shows the separation and the two-dimensional data for the creosote extract using the grating in second order. The inset in Fig. 8 shows the chromatogram obtained for the injected creosote extract. The fluorescence was collected using the UV lens and microscope objective combination shown in Fig. 1, Scheme B. A monochromator slit width of 500 μm was used. Eight of the compounds in the 16 PAH

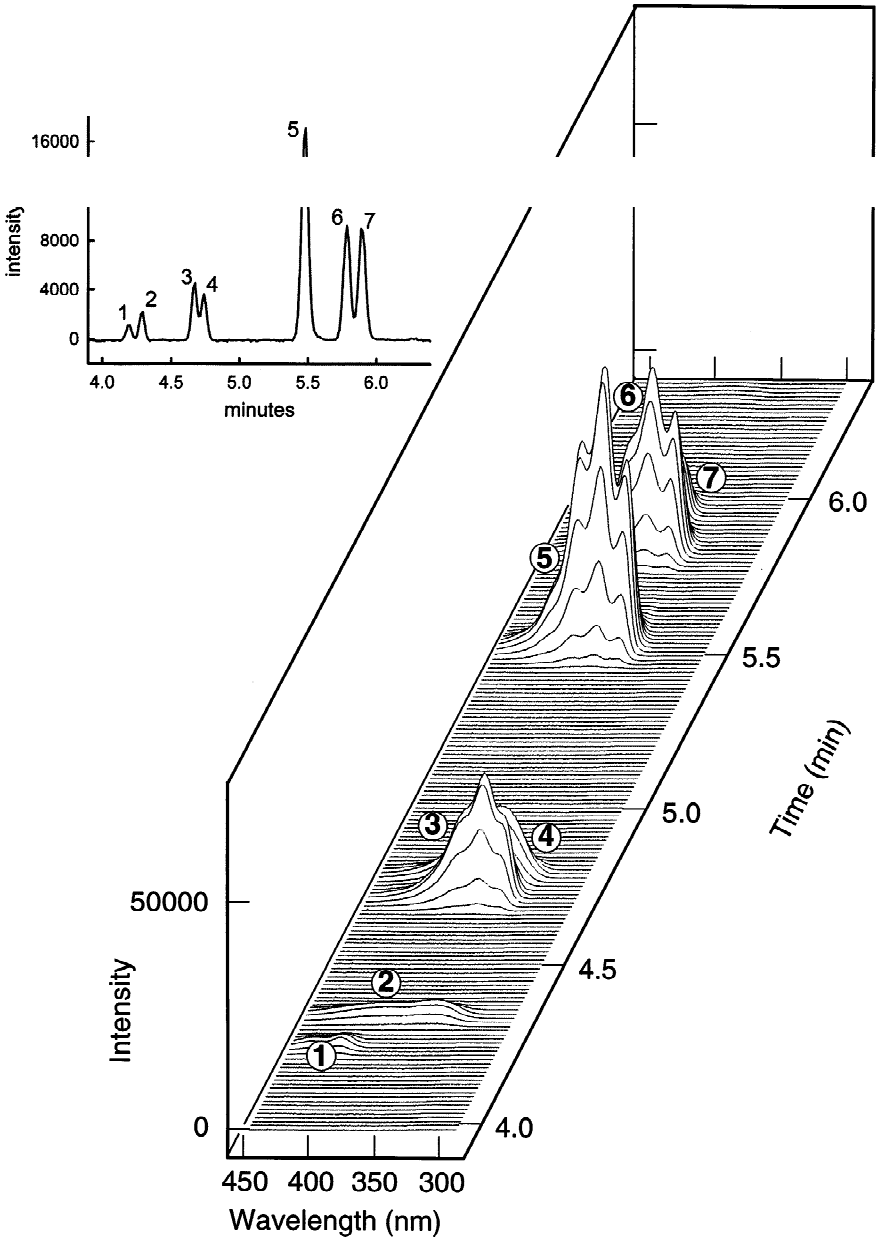

Fig. 6. LIDF spectra and CEC separation of NCAC standards: (1) acridine or degradation product, (2) indole, (3) carbazole, (4) cyanonaphthalene, (5) benzoquinoline, (6) ethylcarbazole, and (7) cyanophenanthrene. Second order dispersed fluorescence collection and a monochromator slit width of 100 μm were used to obtain the spectra. The fluorescence was collected using the UV lens and microscope objective combination shown in Fig. 1, Scheme B. The inset shows the chromatogram obtained by integrating the entire spectral region. The standard solution was separated using a CEC column having a packed length of 30 cm, an applied separation voltage of 25 kV, and a mobile phase composition of 80% ACN and 20% 5 m*M* TRIS. A 5 s, 5 kV electrokinetic injection introduced the sample onto the column.

Table 2
Detection Limits (d.l.) for NCACs using UV-LIDF detection[a]

NCAC (λ_{max})	d.l. ($\times 10^{-10}$ M)
Benzoquinoline (374 nm)	3.62
Ethylcarbazole (374 nm)	0.962
Cyanophenanthrene (370 nm)	1.25

[a] Results were obtained using first order dispersed fluorescence collected from the grating, a 40×-microscope objective as the fluorescence collection optic, a monochromator slit width of 200 μm, and a wavelength integration of 20 nm.

NIST standard mixture were positively identified in the creosote extract using both the dispersed fluorescence results shown in Fig. 8 and the traditional spiking method employed with PMT detection. Only one of the compounds in the NCAC standard mixture was identified using the dispersed fluorescence data; however, the identity of the NCAC in the creosote extract was not confirmed with the spiking technique. With only one efficient separation employing the dispersed fluorescence set-up, one can easily and quickly identify the PAHs and NCAC in the creosote extract without having to perform the task of injecting individual PAHs and NCACs as in the spiking approach. The dispersed fluorescence set-up is shown to rapidly identify polycyclic aromatic compounds in a complex environmental sample.

Figs. 9 and 10 show the separation and identification of PAHs in 2 additional soil extracts. The fluorescence was collected using the UV lens and microscope objective combination shown in Fig. 1, Scheme B. A slit width of 100 μm was used. Fig. 9 shows the separation and the two-dimensional data for a creosote-contaminated soil extract obtained by Soxhlet extraction with dichloromethane. Fig. 10 shows the separation and the two-dimensional data for a PAH-spiked soil extract obtained by sonication. First order dispersed fluorescence was collected from the grating for both environmental samples, showing that peak identification is possible even with the slightly lower spectral resolution compared to second order dispersed fluorescence. The insets in Figs. 9 and 10 show the chromatograms obtained for the injected soil extracts. The results show that the dispersed fluorescence set-up can be used to identify compounds in environmental extracts and that CEC is a robust separation method for separating compounds in real samples, not just standards. The robustness of CEC was also observed during the injection of a total of 12 different extracts (data not shown) onto the same CEC separation column. After all of the soil extract injections, there was no significant loss in resolution observed with the CEC column and several PAHs could be identified in the complex environmental samples.

4. Conclusions

LIDF detection, in combination with CEC, has been shown to be a very powerful analysis approach for the quick identification of PAHs and NCACs in complex environmental samples. The deconvolution of coeluting PAHs demonstrates the power of LIDF detection in identifying compounds quickly based on their different fluorescence spectra even when faced with a separation approach that may not resolve every compound in a mixture. Sensitive LIDF detection should permit the trace analysis of PAHs and NCACs in complex mixtures. In order to take advantage of the improved collection efficiency demonstrated with the microscope objective in comparison to the plano-convex lens and the high sensitivity provided by the LIDF detection technique, it will be necessary to remove the observed background fluorescence resulting from the contaminants of CEC columns. The combined LIDF detection and CEC separation technique should also be very useful in the rapid identification and trace analysis of other natively fluorescent species and species that are tagged with fluorescent labels.

Acknowledgements

The authors thank Gary A. Hux and Judy Rognlien for their technical assistance. The authors also thank Chao Yan and David W. Neyer for helpful discussions. This work was supported by the Laboratory Directed Research and Development program of Sandia National Laboratories. Sandia is a multiprogram laboratory operated by Sandia Corporation, a Lockheed Martin Company, for the United States Department of Energy under contract DE-AC04-94AL85000.

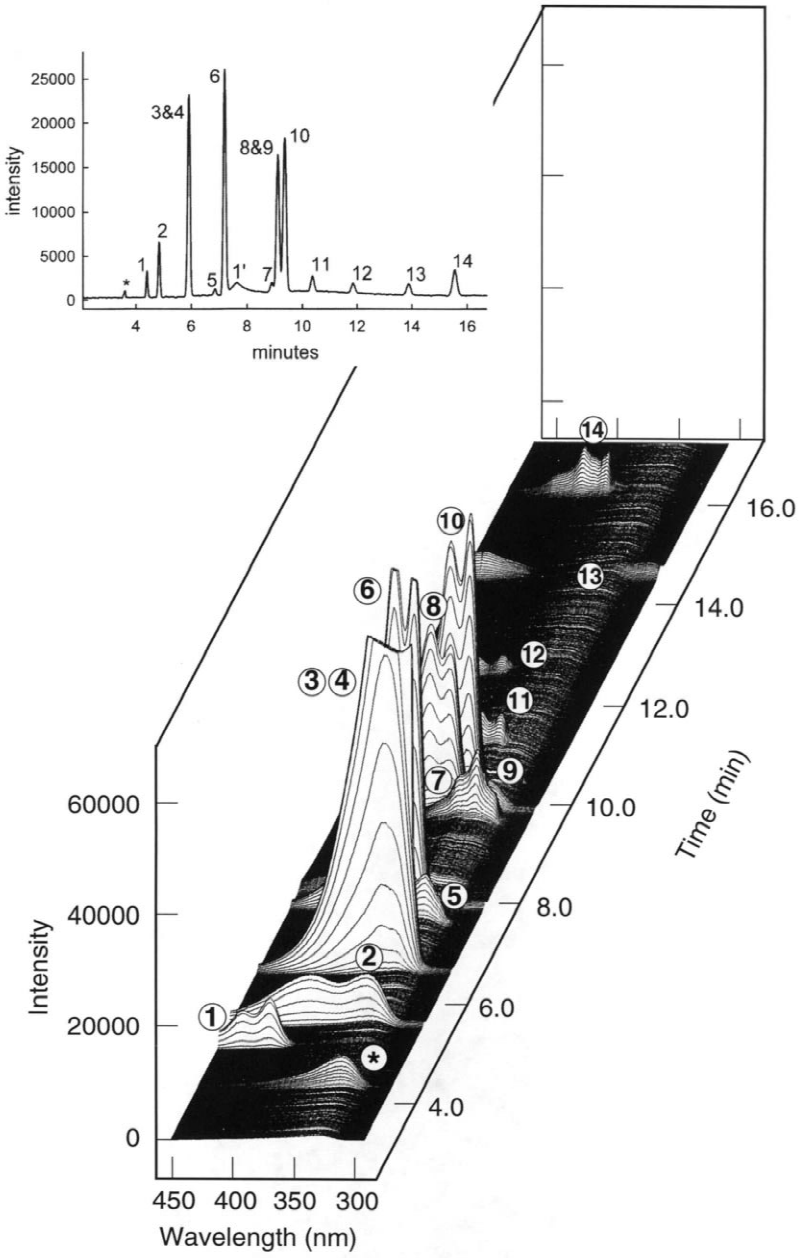

Fig. 7. LIDF spectra and CEC separation of a PAH/NCAC standard mix. Peak identification: (*) impurity, (1,1′) acridine and degradation product, (2) indole, (3) carbazole, (4) cyanonaphthalene, (5) naphthalene, (6) benzoquinoline, (7) acenaphthene, (8) ethylcarbazole, (9) fluorene, (10) cyanophenanthrene, (11) phenanthrene, (12) anthracene, (13) fluoranthene, and (14) pyrene. Second order dispersed fluorescence collection and a monochromator slit width of 100 μm were used to obtain the spectra. The fluorescence was collected using the UV lens and microscope objective combination shown in Fig. 1, Scheme B. The inset shows the chromatogram obtained by integrating the entire spectral region. This standard mix was separated using a CEC column having a packed length of 31 cm and a high voltage of 20 kV applied across the capillary. The mobile phase consisted of 65% ACN and 35% 5 m*M* TRIS and a 5 s, 5 kV electrokinetic injection was used to introduce the sample onto the column.

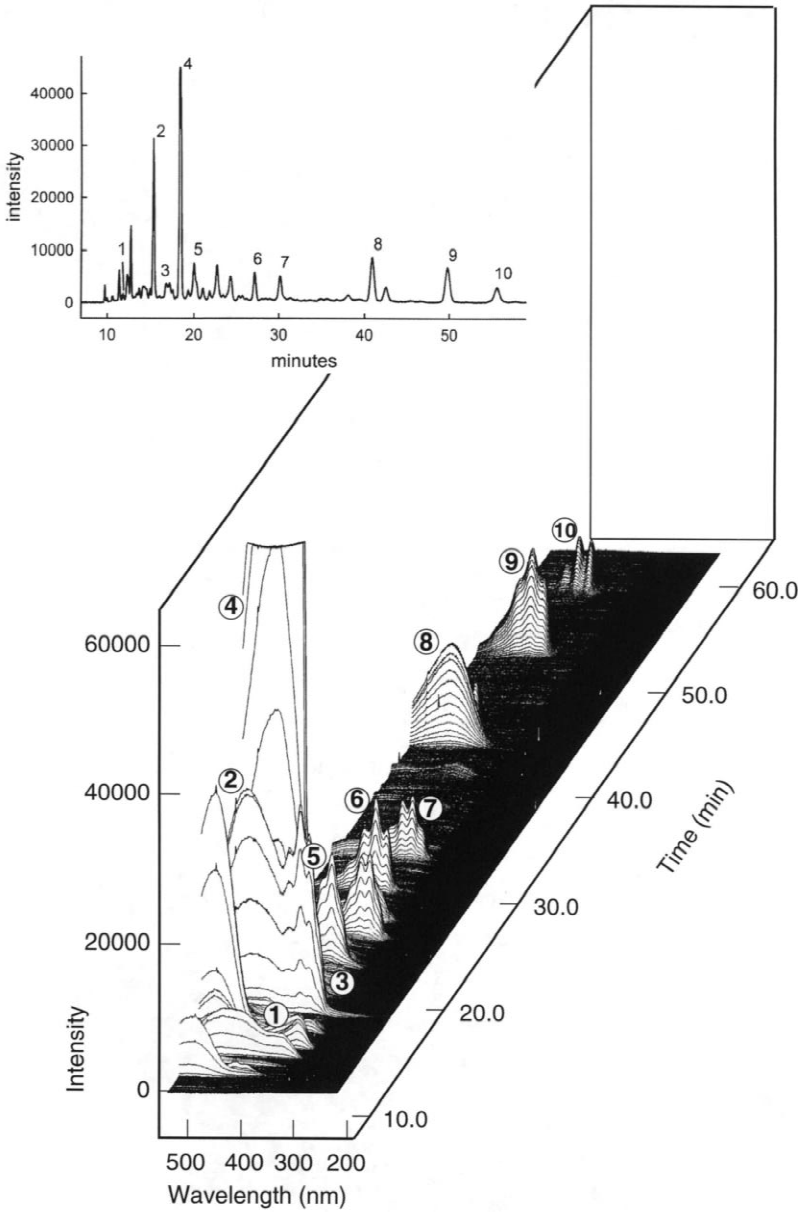

Fig. 9. LIDF spectra and CEC separation of an additional creosote-contaminated soil extract. Peak identification: (1) naphthalene, (2) phenanthrene, (3) anthracene, (4) fluoranthene, (5) pyrene, (6) benz[*a*]anthracene, (7) chrysene, (8) benzo[*b*]fluoranthene, (9) benzo[*k*-]fluoranthene, and (10) benzo[*a*]pyrene. First order dispersed fluorescence collection and a monochromator slit width of 100 μm were used to obtain the spectra. The fluorescence was collected using the UV lens and microscope objective combination shown in Fig. 1, Scheme B. The inset shows the chromatogram obtained by integrating the entire spectral region. The extract was separated using a CEC column having a packed length of 27 cm with a separation voltage of 10 kV applied across the capillary and a mobile phase consisting of 75% ACN and 25% 4 m*M* sodium tetraborate. The extract was introduced onto the column using a 5 s, 5 kV electrokinetic injection.

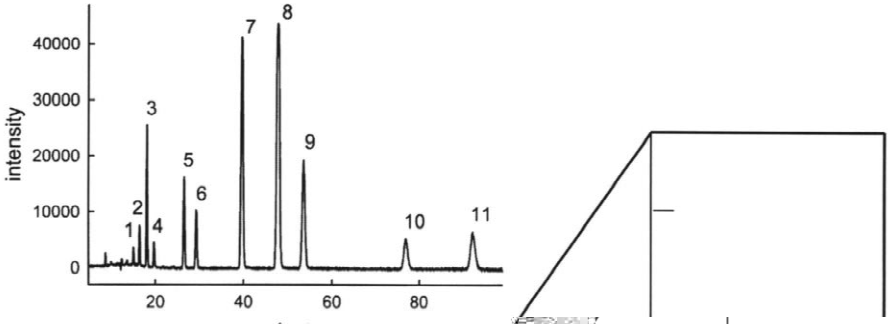

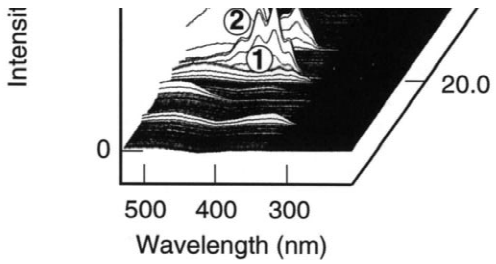

Fig. 10. LIDF spectra and CEC separation of a PAH-spiked soil extract. Peak identification: (1) phenanthrene, (2) anthracene, (3) fluoranthene, (4) pyrene, (5) benz[*a*]anthracene, (6) chrysene, (7) benzo[*b*]fluoranthene, (8) benzo[*k*]fluoranthene, (9) benzo[*a*]pyrene, (10) benzo[*ghi*]perylene, and (11) indeno[1,2,3-*cd*]pyrene. First order dispersed fluorescence collection and a monochromator slit width of 100 μm were used to obtain the spectra. The fluorescence was collected using the UV lens and microscope objective combination shown in Fig. 1, Scheme B. The inset shows the chromatogram obtained by integrating the entire spectral region. The extract was separated using a CEC column having a packed length of 27 cm with a separation voltage of 10 kV applied across the capillary and a mobile phase consisting of 75% ACN and 25% 4 m*M* sodium tetraborate. The extract was introduced onto the column using a 5 s, 5 kV electrokinetic injection.

References

[1] C. Yan, R. Dadoo, H. Zhao, R.N. Zare, D.J. Rakestraw, Anal. Chem. 67 (1995) 2026.
[2] R. Dadoo, R.N. Zare, C. Yan, D.S. Anex, Anal. Chem. 70 (1998) 4787.
[3] W.C. Brumley, C.M. Brownrigg, G.M. Brilis, J. Chromatogr. 558 (1991) 223.
[4] L.A. Colon, Y. Guo, A. Fermier, Anal. Chem. 69 (1997) 461A.
[5] M.M. Dittman, G.P. Rozing, J. Chromatogr. 744 (1996) 63.
[6] G. Ross, M. Dittman, F. Bek, G. Rozing, Am. Lab. 28 (1996) 34.
[7] M.M. Dittman, K. Wienand, F. Bek, G.P. Rozing, LC·GC 13 (1995) 800.
[8] J.H. Knox, I.H. Grant, Chromatographia 32 (1991) 317.
[9] T. Tsuda, Anal. Chem. 59 (1987) 521.
[10] J.W. Jorgenson, K.D. Lukacs, J. Chromatogr. 218 (1981) 209.
[11] V. Pretorius, B.J. Hopkins, J.D. Schieke, J. Chromatogr. 99 (1974) 23.
[12] K.T. Tellman, C.P. Palmer, Electrophoresis 20 (1999) 152.
[13] C.P. Palmer, S. Terabe, Anal. Chem. 69 (1997) 1852.
[14] S.J. Kok, N.H. Velthorst, C. Gooijer, U.A.Th. Brinkman, Electrophoresis 19 (1998) 2735.
[15] A. Kunkel, M. Degenhardt, B. Schirm, H. Watzig, J. Chromatogr. A 768 (1997) 17.
[16] B. Nickerson, J.W. Jorgenson, J. High Resolut. Chromatogr. Chromatogr. Commun. 11 (1988) 533.
[17] D.E. Burton, M.J. Sepaniak, M.P. Maskarinec, J. Chromatogr. Sci. 24 (1986) 347.
[18] N.J. Dovichi, TRACS — Trends Anal. Chem. 3 (1984) 55.
[19] N.J. Dovichi, J.C. Martin, J.H. Jett, R.A. Keller, Science 219 (1983) 845.
[20] M.J. Sepaniak, E.S. Yeung, J. Chromatogr. 211 (1981) 95.
[21] L.W. Hershberger, J.B. Callis, G.D. Christian, Anal. Chem. 51 (1979) 1444.
[22] T. Imasaka, R.N. Zare, Anal. Chem. 51 (1979) 2082.
[23] G.J. Diebold, R.N. Zare, Science 196 (1977) 1439.
[24] F. Andreolini, S.C. Beale, M. Novotny, J. High Resolut. Chromatogr. Chromatogr. Commun. 11 (1988) 20.
[25] J.C. Gluckman, D.C. Shelly, M.V. Novotny, Anal. Chem. 57 (1985) 1546.
[26] Q.S. Hanley, C.W. Earle, F.M. Pennebaker, S.P. Madden, M.B. Denton, Anal. Chem. 68 (1996) 661A.
[27] C.W. Earle, M.E. Baker, M.B. Denton, R.S. Pomeroy, TRAC — Trends Anal. Chem. 12 (1993) 395.
[28] J.V. Sweedler, CRC Crit. Rev. Anal. Chem. 24 (1993) 59.
[29] Y.F. Cheng, R.D. Piccard, T. Vo-Dinh, Appl. Spectrosc. 44 (1990) 755.
[30] P.M. Epperson, J.V. Sweedler, R.B. Bilhorn, G.R. Sims, M.B. Denton, Anal. Chem. 60 (1988) 327A.
[31] J.V. Sweedler, R.B. Bilhorn, P.M. Epperson, G.R. Sims, M.B. Denton, Anal. Chem. 60 (1988) 282A.
[32] R.R. Fuller, L.L. Moroz, R. Gillette, J.V. Sweedler, Neuron 20 (1998) 173.
[33] A.T. Timperman, J.V. Sweedler, Analyst 121 (1996) 45R.
[34] A.T. Timperman, K. Khatib, J.V. Sweedler, Anal. Chem. 67 (1995) 139.
[35] A.T. Timperman, K.E. Oldenburg, J.V. Sweedler, Anal. Chem. 67 (1995) 3421.
[36] J.V. Sweedler, J.B. Shear, H.A. Fishman, R.N. Zare, R.H. Scheller, Anal. Chem. 63 (1991) 496.
[37] C. Borra, D. Wiesler, M. Novotny, Anal. Chem. 59 (1987) 339.
[38] J. Gluckman, D. Shelly, M. Novotny, J. Chromatogr. 317 (1984) 443.
[39] J.C. Gluckman, M. Novotny, J. High Resolut. Chromatogr. Chromatogr. Commun. 8 (1985) 672.
[40] R.D. Jalkian, M.B. Denton, Proc. SPIE 1054 (1989) 91.
[41] J.D. Ingle, S.R. Crouch, Spectrochemical Analysis, Prentice Hall, New Jersey, 1988.